Rheological Properties of Model Alkali-Soluble Associative (HASE) Polymers: Effect of Varying Hydrophobe Chain Length

V. Tirtaatmadja,[†] K. C. Tam,[*,†] and R. D. Jenkins[‡,§]

School of Mechanical and Production Engineering, Nanyang Technological University, Nanyang Avenue, Singapore, and UCAR Emulsion Systems, Research and Development, Union Carbide Corporation, Cary, North Carolina 27511

Received August 9, 1996; Revised Manuscript Received December 20, 1996[⊗]

ABSTRACT: The rheological properties of 1 wt % aqueous solutions (at pH between 8.7 and 9.5) of model associative (HASE) polymers are presented. These polymers are the polymerization product of methacrylic acid, ethyl acrylate, and macromonomers which contain hydrophobes with the alkyl chain ranging in length from C_{12} to C_{20}. At high pH, the polymers form a network of temporarily associating hydrophobic junctions, resulting in an enhancement of the shear viscosity which increases with the hydrophobe chain length. Strain amplitude sweep results show that the strength of the hydrophobic association increases with the length of the hydrophobe. This is also reflected in the increase in the ratio of the elastic to viscous components of the linear viscoelastic properties. When sheared beyond its equilibrium state, the associative polymers display a terminal (second-order) viscoelastic behavior at higher frequencies as the network is increasingly being disrupted by higher applied stresses. The general behavior of the polymers changes from Zimm-like to Rouse-like, and to reptation-type with a crossover between the storage and loss moduli curves, as the alkyl chain of the hydrophobes increases from 12 to 16, and to 20, carbon atoms. It is believed that in the unstressed state, other relaxation processes with much longer times are involved, and it is these long relaxation times which are greatly curtailed as the network is disrupted by an applied stress.

1. Introduction

Water soluble, hydrophobically modified polymers are being used increasingly in a wide range of industrial applications, including paint formulations and paper coatings. In paint formulation, these polymers are used as thickeners to increase the low shear viscosity, to prevent pigment settling during storage, and to instill a suitable pseudoplastic and thixotropic behavior for proper application at high shear rates. The particular class of hydrophobe-modified, alkali-soluble (HASE) polymers commands a special interest due to its low cost of production and ease of handling and utilization. These are long chain acrylic polymers interspersed with carboxylate groups, having hydrophobe end-capped macromonomers distributed along the chain. In the emulsion state, at low pH, the polymers are in the form of water-insoluble latexes. Upon neutralization to a pH greater than 7, the polymers become water soluble due to carboxylate repulsion of the anion backbone.[1]

The main microstructural characteristic of this polymer system is the formation of both intra- and intermolecular hydrophobic associations in aqueous solutions.[2] In the concentration range of industrial interest, the intermolecular interactions are predominant and they form a temporary network of associating hydrophobic junctions. The linear and nonlinear viscoelastic behavior of these associating polymers is expected to be complex and depends on a number of factors, such as the structure and composition of the polymer backbone, its water solubility and glass transition temperature, the structure and concentration along the backbone of the hydrophobic macromonomers, and the structure of the hydrophobes.[1] Due to the complexity, it is appropriate to investigate model associative polymers whose structural parameters can be specifically modified, in order to understand, from fundamental first principles, the relationships between structure and rheological behavior. This would form a basis for the understanding of the mechanism of rheology modification by this class of associative polymers.

This article presents some results on the effect of varying the length of the hydrophobes on the rheological behavior of model HASE associative polymers. It is found that by varying the length of the hydrophobic group, the rheological properties of the model polymers are drastically altered, with the behavior observed resembling certain well-known classical theories. These theories are described in section two, while the results and the fitting of the theories to the results are presented in section four. The interpretations of the results in terms of the network structure of the polymers in solution are presented in section five.

2. Theoretical Consideration

One of the most widely used molecular models for representing polymeric systems is the bead−spring model, of which Rouse[3] and Zimm[4] are two well-known examples. These models have been introduced for dilute solutions of linear flexible coils where sections of the molecules, or monomer units, are represented by beads joined together by Hookean springs. In the Rouse model, hydrodynamic interaction caused by the motion of neighboring submolecular junctions is ignored; this corresponds to the "free-draining" assumption used in the calculations of intrinsic viscosity.[5] This theory is based on the change in the free energy associated with the entropy decrease of the molecules when disturbed from its equilibrium, random conformations and the tendency of the system to diffuse back toward a random state due to Brownian motions.

In the theory of Zimm, frictional resistance to the motion of the beads in the bead−spring chain and the viscous drag from other beads in the same chain is

* To whom correspondence should be addressed.
† Nanyang Technological University.
‡ Union Carbide Corp.
§ Present address: Union Carbide Asia Pacific, Inc., Technical Center, 16 Science Park Dr., The Pasteur, Singapore 118227.
⊗ Abstract published in *Advance ACS Abstracts,* May 1, 1997.

S0024-9297(96)01202-8 CCC: $14.00

included, hence the term "dominant hydrodynamic interaction". In this treatment, the force on each bead is calculated as the sum of the hydrodynamic drag force from the solvent, the force associated with Brownian motion and the Hookean spring forces exerted by the two neighboring beads connected to it. Although derived from a different approach, the Rouse theory and the limiting case of Zimm in which hydrodynamic interaction is neglected gives the same linear viscoelastic results. For both theories, the frequency dependence of the dynamic shear moduli $G'(\omega)$ and $G''(\omega)$ can be expressed in the following forms:

$$G'(\omega) = G_0 \sum_{k=1}^{N} \frac{\omega^2 \lambda_k^2}{1 + \omega^2 \lambda_k^2} \tag{1}$$

and

$$G''(\omega) - \omega\eta_s = G_0 \sum_{k=1}^{N} \frac{\omega\lambda_k}{1 + \omega^2 \lambda_k^2} \tag{2}$$

where G_0 is the relaxation modulus, λ_k is the kth mode of relaxation time, and N is the number of monomer units. Alternatively, these functions can be represented in terms of the reduced moduli:

$$G'_R(\omega_R) = \frac{G'(\omega)}{G_0} = \sum_{k=1}^{N} \frac{\omega_R^2(\lambda_k/\lambda_1)^2}{1 + \omega_R^2(\lambda_k/\lambda_1)^2} \tag{3}$$

and

$$G''_R(\omega_R) = \frac{G''(\omega) - \omega\eta_s}{G_0} = \sum_{k=1}^{N} \frac{\omega_R(\lambda_k/\lambda_1)}{1 + \omega_R^2(\lambda_k/\lambda_1)^2} \tag{4}$$

where ω_R is the reduced frequency of oscillation, i.e. $\omega_R = \omega\lambda_1$, where λ_1 is the longest relaxation time of the Rouse/Zimm theory.

The difference between these two models lies in the spacing of their relaxation times. For the Rouse model, the spectrum of relaxation times can be obtained from

$$\lambda_k = \frac{6(\eta_0 - \eta_s)}{\pi^2 k^2 G_0} \tag{5}$$

and for the Zimm model,

$$\lambda_k = \frac{1.71(\eta_0 - \eta_s)}{E_k G_0} \tag{6}$$

where η_0 and η_s are the solution and solvent viscosities, respectively. The approximate values of E_k for $0 < k < 7$ are given by Zimm et al.[6] and for large k (≥ 7),

$$E_k \approx \frac{\pi^2 k^{3/2}}{2}\left(1 - \frac{1}{2\pi k}\right) \tag{7}$$

For these two molecular theories, the viscoelastic behavior at low frequencies is typical of a second-order fluid; that is, the G' curve follows a second-order behavior with respect to frequency and G'' is directly proportional to frequency, such that the dynamic viscosity is constant in the low-frequency range. At higher frequencies, the Rouse theory predicts G' and $G'' - \omega\eta_s$ to be equal and proportional to $\omega^{1/2}$, while the prediction of the Zimm theory shows G' and $G'' - \omega\eta_s$ to be parallel and proportional to $\omega^{2/3}$, the values differing by a factor of $\sqrt{3}$.

Although these molecular models have been derived on the basis of conditions of very dilute to infinitely dilute solution, it has been found experimentally that both Zimm-like and Rouse-like behavior has been observed for solutions of polystyrene of narrow molecular weight distribution at finite concentrations, in the range sometimes described as "semidilute",[7] as well as for solutions for poly(acrylamide).[8] In these cases, the change from Zimm-like to Rouse-like behavior occurs as both the concentration and molecular weight of the polymer increases. At still higher concentrations or molecular weight, where entanglement between portions of the polymer chains becomes evident, viscoelastic behavior of the polymer solutions is found to be entirely different and regions in which G' is actually larger than $G'' - \omega\eta_s$ are observed.[9]

In an entangled system, the polymer chain can be visualized as being constrained within a fictitious tube formed by the surrounding molecules at entangled points, and the polymer chain diffuses by wormlike motion through this tube. The tube is continuously being renewed as the chain ends explore new paths through the obstacle lattice. This is the reptation model first introduced by DeGennes.[10] The polymer chain has to undergo a reptating motion through the tube in order to disentangle. Doi and Edwards[11] applied the reptation model to the dynamics of entangled polymers and considered a primitive path confined by slip-links that segmented the entrapped chains. When a deformation is imposed, the isotropic stress is dissipated through the reptation of the chains in the confining tube and by a Rouse-type relaxation of segments held between entangled points. The relaxation time of polymers by the reptation process is expected to be orders of magnitude larger than the segmental relaxation and would dominate the terminal behavior of the polymers. The linear viscoelastic behavior in this region is given by the following:

$$G'(\omega) = G_0 \sum_{k;\text{odd}} \frac{8}{\pi^2}\frac{1}{k^2}\frac{\omega^2\lambda_k^2}{1 + \omega^2\lambda_k^2} \tag{8}$$

and

$$G''(\omega) = G_0 \sum_{k;\text{odd}} \frac{8}{\pi^2}\frac{1}{k^2}\frac{\omega\lambda_k}{1 + \omega^2\lambda_k^2} \tag{9}$$

where

$$\lambda_k = \frac{\lambda_1}{k^2} \qquad k = 1, 3, 5, \ldots \tag{10}$$

At high frequencies the Doi−Edwards model predicts a plateau in the G' curve and G'' which decreases in value with frequency.

3. Experimental Section

3.1. Materials Used. The model associative polymers studied are hydrophobically modified, alkali-soluble emulsions (HASE) synthesized by Union Carbide. The chemical structure of these associative polymers is shown in Figure 1, and their compositions are given in Table 1. The polymers are the

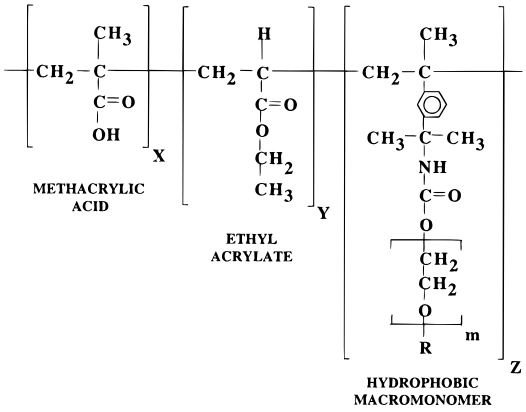

Figure 1. Chemical structure of the model HASE associative polymers.

Table 1. Composition of the Model Associative HASE Polymers

polymer designation	hydrophobe name	hydrophobe formula	weight fraction MAA/EA/AM	molar fraction MAA/EA/AM
RDJ31-1	none		45.00/55.00/0	48.76/51.24/0
RDJ31-3	dodecyl	$C_{12}H_{25}$	38.52/45.70/15.78	49.05/50.05/0.90
RDJ31-4	hexadecyl	$C_{16}H_{33}$	38.40/45.56/16.04	49.06/50.04/0.90
RDJ31-5	eicosanyl	$C_{20}H_{41}$	38.14/45.25/16.61	49.06/50.04/0.90

Table 2. Composition of the Surfactant Precursors and Macromonomers Used for Synthesis of the Model Associative HASE Polymers

hydrophobe name	hydrophobe formula	n	hydroxyl M_n	m	macrom M_n (calculated)	GPC M_n/M_w
dodecyl	$C_{12}H_{25}$	11	1726	35	1927	2120/2179
hexadecyl	$C_{16}H_{33}$	15	1761	35	1962	2197/2257
eicosanyl	$C_{20}H_{41}$	19	1835	35	2036	2023/2077

emulsion polymerization product of methacrylic acid (MAA), ethyl acrylate (EA), and what we call an "associative macromonomer" (AM). The associative macromonomers comprise a poly(oxyethylene) chain connected to an alkyl (hydrophobic) group at one end and a vinyl polymerizable group at the other end. They are prepared by first ethoxylating a linear alkyl primary alcohol to make a surfactant and subsequently reacting the resultant terminal primary hydroxyl group of the ethoxylated chain portion of the surfactant with an unsaturated isocyanate. This connected the ethoxylated portion of the surfactant to a vinyl polymerizable double bond through a urethane linkage. In this study, three linear alkyl primary alcohols, namely, *n*-dodecanol (C_{12}), *n*-hexadecanol (C_{16}), and 1-eicosanol (C_{20}), have been ethoxylated to circa 35 mol of ethylene oxide, i.e. $m = 35$, and reacted with the unsaturated isocyanate, known by the trade name TMI (meta).

When the associative macromonomer is copolymerized with methacrylic acid and ethyl acrylate, the resulting polymer has a backbone that consists of MAA, EA, and the residue of the vinyl group of the associative macromonomer, as well as flexible, water-soluble side chains that are terminated by a linear alkyl hydrophobic group. For the series of associative polymers studied in this work, the mole fractions of MAA/EA/macromonomer were kept constant (see Table 1), so that the only difference among the various polymers was the length of the hydrophobic groups of the macromonomers, this ranges from C12 to C20. Note that we have included in the series the control polymer RDJ31-1 which contains no associative macromonomer. A detailed description of the synthesis procedure is as follows.

Macromonomer Synthesis. Surfactant precursors for the macromonomers were prepared by reacting ethylene oxide with one of the alcohols listed in Table 2, according to

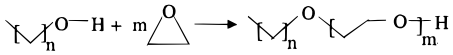

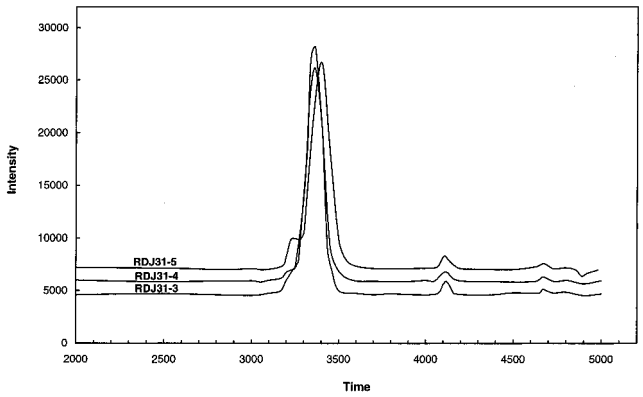

Figure 2. Gel permeation chromatography charts of macromonomers for model associative polymers RDJ31-3, -4, and -5.

The alcohols, used as received without further purification, were ethoxylated in a pressure autoclave at 140 °C and 70 psi using 0.25% potassium hydroxide (based on total reaction mass) as catalyst. Ethylene oxide was added in small aliquots to keep the reaction temperature and pressure constant. After complete addition of the ethylene oxide, the reaction mixture was held at the temperature and pressure to ensure complete conversion of ethylene oxide. The liquid product was poured from the reactor hot and had only a slight trace of amber color. The product solidified on cooling to room temperature. Its molecular weight was measured by end group analysis (hydroxyl number). The titration of the hydroxyl end groups provides a measure of the absolute number average molecular weight of the surfactant (see Table 2). The molecular weight distributions of the samples (i.e. polydispersity) were measured by gel permeation chromatography using tetrahydrofuran solvent. The molecular weights obtained are relative to polystyrene standards and were used for assessing the breadth of the distribution and for relative comparisons only (see Table 2). The number average molecular weights obtained by hydroxyl number analysis were used in subsequent calculations.

Associative macromonomers were prepared by reacting the surfactant precursors with a stoichiometric amount of *m*-TMI (dimethyl-*m*-isopropenylbenzyl isocyanate), based on the hydroxyl number average molecular weight of the surfactant, according to

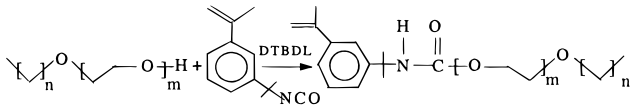

The surfactant was melted and heated to 85 °C under nitrogen purge to prevent decomposition. Once melted, 0.1% dibutyltin dilaurate (DTBDL) catalyst (based on total reaction mass) was added to the reaction mixture and allowed to mix thoroughly. Then, the *m*-TMI was added, and after the initial exotherm (typically 7 °C), the reaction mixture was held at 85 °C for another 4 h to ensure complete conversion of the isocyanate. The product was packaged in a jar while hot, and solidified on cooling to room temperature. The molecular weight and molecular weight distributions of the macromonomers were measured by gel permeation chromatography; the GPC results, shown in Table 2 and Figure 2, indicate a narrow distribution of the molecular weights for all three macromonomers and that the reaction proceeds to completion, as the molecular weights are very close to within approximately 10% of the expected values. (Note that the molecular weight of the macromonomer used to calculate the fractions of ethyl acrylate, methacrylic acid, and macromonomer used in subsequent emulsion polymerization was calculated by adding the molecular weight of *m*-TMI, i.e. 201.25, to the hydroxyl number average molecular weight of the surfactant precursor.)

Emulsion Polymerization. The weight fractions of the methacrylic acid, ethyl acrylate, and macromonomer used to

prepare the final model alkali-soluble hydrophobic associative polymers are shown in Table 1. A typical standard semibatch emulsion polymerization process is described below.

A monomer mixture (of total weight of 620 g) was prepared by charging ethyl acrylate, methacrylic acid (both from Aldrich Chemical Co.), and macromonomer, in the proportions shown in Table 2, plus 26 g of a 75% solution of Aerosol OT surfactant (American Cyanamid Co.) and 60 g of distilled deionized water to a bottle, and the content was dispersed by vigorous shaking. This monomer mixture was then charged to a 1-L graduated monomer feed cylinder. An initiator feed mixture comprising 8 g of sodium persulfate (Aldrich Chemical Co.), 2 g of sodium bicarbonate (Aldrich Chemical Co.), and 45 g of distilled deionized water was prepared in another container and was charged to a (100-mL) syringe pump. In a third container, 16 g of sodium persulfate was dissolved in 40 g of water to form the initial catalyst solution. To the reaction vessel (a 3-L resin flask), were charged 1377 g of distilled deionized water, 5.3 g of 2-sulfoethyl methacrylate (Hampshire Chemical Co.), and 5.3 g of a 75% solution of Aerosol OT surfactant. Under nitrogen purge, the reactor was heated to 80 °C, whereupon 68 g of the monomer mixture was added. When the reactor temperature reached 80 °C, the catalyst solution was added to the reactor to initiate polymerization. After the initial monomers had reacted for 30 min to form an in-situ seed product, the remaining monomer and initiator feed mixtures were conveyed to the reaction vessel at a rate of 4.5 and 0.4 g/min, over a 2-h and a 2.5-h period, respectively, while the reaction mixture was under continuous stirring at a reaction temperature of 80 °C. The reaction was left to proceed for another hour for residual monomers to react, after which the solid product was cooled and filtered through a 200-mesh Nylon cloth. The final solid content of the polymers was approximately 30% by weight. These values were subsequently confirmed by drying the product in an oven at 80 °C and weighing.

The polymer latexes obtained from the emulsion polymerization process were dialyzed in regenerated cellulose membrane tubes for approximately 4 weeks, with frequent changing of water, and the solid content of each polymer in the series was again determined by drying (in an oven at 80 °C) and weighing. Stock solutions containing 5 wt % of the solid latexes were made up, from which the final solutions of 1.0 wt % polymers were prepared. (Note that all associative polymer solutions used in this study have been prepared in deionized water containing 10^{-4} M of KCl.) The 1 wt % polymer solutions were neutralized with NaOH solution to pH 8.7 (except for the RDJ31-5, which was at pH 9.5). Upon neutralization, the methacrylic acid is ionized and the electrostatic repulsive force of the negative charges along the chain backbone causes the chain to expand, resulting in the solubilization of the polymers in aqueous solutions at high pH. The expansion of the MAA/EA chains promotes the formation of both intra- and intermolecular associations of the hydrophobic groups. The resultant clear solutions of the various polymers can be seen to possess a wide range of viscosities, depending on the hydrophobe chain length, as will be shown in the next section. For the RDJ31-3, -4, and -5 polymers, formation of hydrophobic associations with neighboring chains are facilitated by the relatively long ethylene oxide linkages of the hydrophobic groups. The effect of ethylene oxide chain length on the hydrophobic association and its effect on the solution viscosity is currently under investigation in our laboratory.

The molecular weight of the polymers is unknown at this stage, but it is being determined in our laboratory using the light scattering technique, although it should be pointed out that the procedure is not straightforward due to the associative nature of the hydrophobic groups, and the use of solvent and surfactant to mask the hydrophobes from associating with others is being investigated. However, the variation in MW across the series of polymers containing increasing hydrophobe alkyl chain length is expected to be minimal due to two major factors. Firstly, the amount of hydrophobic macromonomers incorporated into the polymers was less than 1 mol % of the total components. Secondly, the synthesis procedure was identical for all the polymers (including the control), with the feed mixture being charged into the reactor at the so-called "monomer-starved" conditions. Under these conditions, the instantaneous composition of the polymer is expected to be the same as that of the monomer feed. From the published reactivity ratios of (meta) TMI in ethyl acrylate (i.e. $r_1 = 0.74$ and $r_2 = 0.17$), and by assuming that the poly(ethylene oxide) and hydrophobe portion of the macromonomer has minimal impact on these ratios, then the incorporation of the hydrophobic macromonomers via the double bond of the isocyanate is expected to be fairly random. Moreover, the intrinsic viscosity results of the associative polymers and the control determined in the presence of SDS at a concentration of 0.05 M, which is in excess of the critical micelle concentration (CMC) of the surfactant, show that the values are very similar. It thus indicates that the molecular weights of the polymers with different hydrophobe alkyl chain lengths and of the control polymer must be close to each other.

Additionally, for the control polymer, in the neutralized state, the viscosity average molecular weight has been estimated from the intrinsic viscosity data obtained in 0.01 and 0.1 M NaCl solutions,[12] using the Mark−Houwink constants for the sodium salt of poly(acrylic acid) in 0.01 and 0.1 M NaBr solutions,[13] respectively. The value was found to be of the order of 200 000. As stated previously, the molecular weight of the associative polymers and the control is expected to be similar in magnitude; thus, based on the MW of 200 000, $Z = 0.9$, and $m = 35$ (see Figure 1 and Tables 1 and 2), the number of hydrophobic macromonomers is estimated to be approximately 18−20 per chain.

At a concentration of 1 wt %, the polymers are probably in the semidilute state, as the viscosity results as a function of concentration for the control polymer indicate when considered in the light of recent work on polyelectrolyte solutions.[14]

We would also like to point out that the rheological properties of model associative polymer RDJ31-4 presented in this work have been obtained from a solution which was 1-month old, and comparison of the results obtained from freshly prepared sample shows some differences in the rheological data. This will be discussed further in the Results.

3.2. Experimental Technique. The rheological properties of the associative polymer solutions were measured using a controlled stress Carri-Med model CSL500 rheometer and a controlled rate Contraves LS40 rheometer. For the Carri-Med CSL500, two geometries, a cone-and-plate fixture (with a 40 mm, 2° cone) and a double-gap concentric cylinder (with an inner cup diameter of 40 mm and both radial gaps of 0.34 mm), were used. For the Contraves LS40, a concentric cylinder (with an outer cup diameter of 12 mm and a gap of 0.5 mm) was used. The Contraves LS40 and the Carri-Med CSL500 with the double-gap concentric cylinder were used for the measurements of the less viscous solutions of RDJ31-1, -3, and -4. The steady shear and dynamic results obtained from both instruments agree very well with each other, with the Contraves being capable of measurements to lower shear rates. For the more viscous solution of RDJ31-5, the cone-and-plate system on the Carri-Med was used. The results for the RDJ31-5 solution are the same as those presented in our previous paper.[15]

In addition to steady shear and oscillatory flow measurements, the technique of superposition of oscillation on steady shear flows presented previously[15] was applied to the three solutions having hydrophobic macromonomers attached to the polymer backbone, i.e. RDJ31-3, -4, and -5, in order to probe the network structure at various applied stress conditions. The technique was only possible with the controlled stress rheometer. A detailed discussion of the superposition technique, together with a schematic diagram depicting the stress and strain curves involved, is given in our previous paper.[15] It is hoped that the results obtained from superimposing oscillations at different frequencies onto steady shear flows will prove useful as a means of studying the structure of the associative polymers when subjected to various shear conditions.

In this work the rheological measurements were carried out at 25 ± 0.1 °C. The effect of shear history has been found to be significant for the more gel-like solutions of RDJ31-4 and

-5, requiring several minutes after the cessation of shear to restore to its equilibrium state, while this effect becomes less critical for the less viscous solutions of RDJ31-1 and -3. Hence all solutions of associative polymers investigated were subjected to the same preshearing at a rate of 10 s^{-1} for 5 min, followed by a 5-min rest period prior to each set of measurements. Strain amplitude sweeps were also carried out at various applied shear stresses at frequencies of 1, 10, and 100 rad/s, to determine the range of strain within which linear viscoelastic response of the dynamic storage and loss moduli can be obtained. Subsequent dynamic measurements were carried out within this linear region.

4. Results

All the associative polymers, as well as the control RDJ31-1, show an increase in shear viscosity upon neutralization.[12,16] Shear viscosity of the solutions rises sharply at pH 6 and reaches an almost constant value at pH 7 and above. As the methacrylic acid comprising the backbone of the polymers is ionized, the electrostatic repulsive force due to negative charges along the chain causes it to expand, hence increasing its hydrodynamic volume in solution. In the semidilute solution state, the increase in the hydrodynamic volume due to Coulombic repulsion is sufficient to cause the viscosity of even the control RDJ31-1 to significantly increase beyond the value found in its natural state at low pH. For the other polymers containing hydrophobic macromonomers, the expansion of the chain backbone at high pH consequently allows a significant crossover from the predominantly intramolecular associations of hydrophobic groups from within the same polymer chain to more intermolecular associations of hydrophobes from neighboring chains. The associative polymers thus form a network of associating junctions in solutions at high pH and a far more dramatic increase in the viscosity is encountered (see Figure 4).

The aggregation number of the hydrophobic groups which associate to form junctions is currently being studied by Winnik's group at the University of Toronto, using the fluorescence spectroscopy techniques. For the HEUR type of nonionic asssociative polymer with alkyl hydrophobes attached to both ends of the long chain poly(ethylene oxide), the aggregation number has been found to be 28 ± 3 for the $C_{12}H_{25}$ hydrophobe[17] and 22 ± 2 for the $C_{16}H_{33}$ hydrophobes,[18] using the fluorescence probe technique. However, an alternative technique such as neutron scattering performed on polymers with deuterated end groups have also been used with success.[19] These hydrophobes are the same as the RDJ31-3 and -4 polymers, respectively; however the aggregation number for the HASE polymers is expected to be lower due to their bulkier backbones, as well as the difference in the hydrophobicity of the associating groups, as will be discussed later. This number also depends on the size and, hence, strength of the hydrophobic moieties. The hydrophobes forming the associating junctions are most likely to be both from within the same chain and from neighboring chains. Placing the hydrophobic group at the end of a relatively long and flexible side chain, i.e. the poly(ethylene oxide) spacer, facilitates associations since this allows the hydrophobe to diffuse to association clusters without being hindered by the diffusion of the polymer backbone.[1] The resultant structure of these associative polymers in solution at high pH is a network of temporary junctions of hydrophobes, which dissociate and reassociate dynamically. The extent of the network is expected to depend on both the junction density and the strength of the hydrophobic association, as found with the linear end-capped HEUR

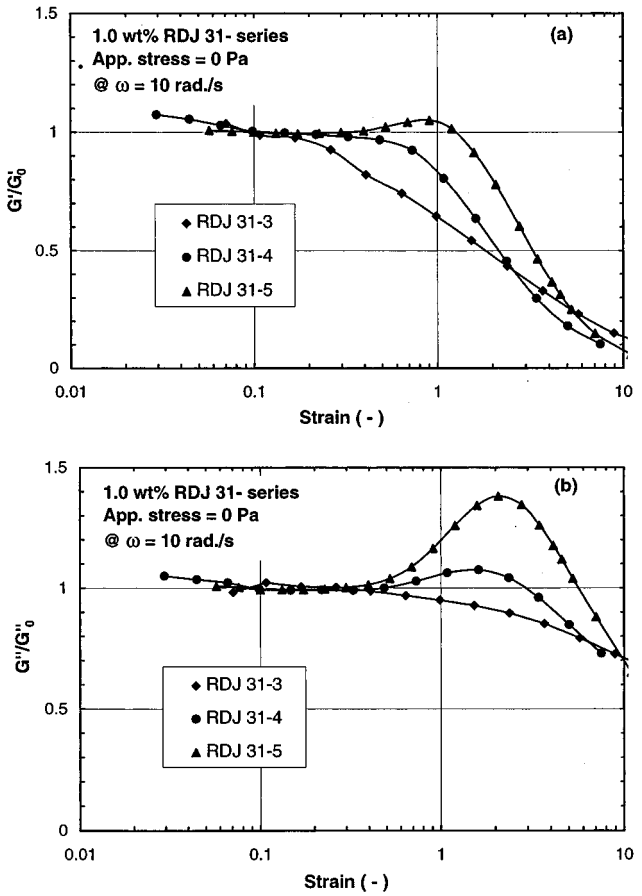

Figure 3. Strain amplitude sweep results of the 1 wt % solutions of RDJ31-series polymers at an angular frequency of 10 rad/s: (a) normalized storage modulus; (b) normalized loss modulus.

systems.[20−22] At higher pHs, beyond 10, there appears to be a slight decrease in the viscosity of the solutions; this is believed to be due to partial shielding of negative charges along the polymer backbone in the presence of excess Na^+ ions, causing the polymer chains to contract slightly with a possible reduction in the amount of intermolecular hydrophobic associations, and hence the viscosity.[23] The solutions of associative polymers in the pH range between 8.5 to 10 are unaffected by the variation in pH.

4.1. Association Strength. The relative strength of the network junctions of the three associative polymers can be qualitatively compared by observing the strain amplitude sweep results, a technique also advocated for differentiating between strong and weak gels.[24] The elastic and viscous components of the dynamic shear moduli, G' and G'', for the unsheared state of these polymers at a frequency of 10 rad/s are plotted against strain in Figure 3a,b, respectively, where the data have been normalized with respect to their corresponding linear viscoelastic values. For RDJ31-3 having the shortest alkyl chain of $C_{12}H_{25}$, the dynamic properties, especially the storage modulus, decrease dramatically when the strain amplitude is increased beyond a certain value. The network structure of RDJ31-3 is severely ruptured at a much lower strain compared to that for the other two polymers with longer hydrophobes, indicating that the strength of its hydrophobic associations is the weakest among the three associative polymers. For RDJ31-3, the drop in the G' values is not immediately accompanied by a drop in the G'' values, as the breaking of the network junctions does

not necessarily lead to a reduction in the effective volume of the network until at a higher strain when the network is sufficiently disrupted.

The association strength of both RDJ31-4 and -5 is much higher than for RDJ31-3, as can be seen in the increase in the G'', and a smaller increase in G' values, with increasing strain amplitude. The increase in G'' can be attributed to an increase in the effective volume of the network structure in solution, as a result of the extension of both the hydrophobic side chain and the polymer chain backbone as the oscillation strain is increased. This increase is only observed when the relaxation time of the network is longer than the time per cycle of oscillation, that is, when the polymer network does not have sufficient time to relax to its equilibrium state within each oscillation cycle. On the other hand, the slight but discernible increase in the G' values of RDJ31-5 indicates that there is possibly an increase in the network junction density due to enhanced intermolecular associations. It may also be a result of the nonlinear response of the spring (in an analogy to the (mechanical) spring-and-dashpot model), as it is stretched beyond the linear or Hookean limit.[25] In this case the network junctions must be sufficiently strong to support the stress at high extension before failure occurs. The fact that the increase in both moduli is larger for RDJ31-5 compared to RDJ31-4 clearly indicates that the strength of the hydrophobic association, and the binding strength of the hydrophobes in a junction, increase with the length of the alkyl chain. The decrease in both G' and G'' at very high strain is due to an en mass destruction of the network junctions and the ultimate rupturing of the network.

4.2. Steady Shear Results. Steady shear viscosities of the associative polymers with different hydrophobe chain lengths are shown in Figure 4a,b as a function of shear stress and shear rate, respectively. Although increased significantly beyond its unsolubilized state, the viscosity of the 1 wt % solution of RDJ31-1 remains essentially Newtonian. On the other hand, the other three polymers which contain hydrophobic groups of various lengths show large low-shear viscosities and a highly shear-thinning behavior, a characteristic typical of associative thickeners with a comb-type structure, i.e. with hydrophobes attached along the main chain backbone.[1,2,26] The low-shear viscosity values of these polymers show a rise of between 2 and 3 orders of magnitude as the hydrophobic chain length increases from C_{12} to C_{20}. The viscosity profiles of these associative polymers display one or more inflection points, which can be clearly discerned when plotted against shear stress; this behavior is not usually observed in conventional entangled polymer systems. The decrease in the viscosity with increasing shear stress is due to the disruption of the network junctions; that is, the rate of junction disruption exceeds the rate at which hydrophobic associations can be re-formed. The stress required depends on the strength of the associating hydrophobic junctions, with RDJ31-5 remaining at a constant viscosity up to a relatively high stress of 1 Pa, while RDJ31-3 and -4 shear-thin at an applied stress less than 0.01 and 0.1 Pa, respectively.

The low-shear viscosities of the polymers are plotted as a function of the number of carbon atoms in the hydrophobe in Figure 5, with the dotted line drawn only as a guide to join the points. For the three associative polymers with C atoms in the hydrophobes increasing from 12 to 20, the low-shear viscosity increases exponentially with the number of C atoms, at a fixed degree of ethoxylation. This is consistent with the finding of Annable et al.[20] for the hydrophobically end-capped HEUR polymers with varying hydrophobe chain lengths from C_{12} to C_{22}. From the slope of the line in Figure 5, the value of the activation energy of dissociation can be estimated to be approximately 0.6 kT per each increment in C atom, where k is the Boltzmann superposition constant and T is the absolute temperature. This value is somewhat lower than that found by Annable and his co-workers for their HEUR system (i.e. 1 kT). In fact, the activation energy value obtained from the hydrophobe chain length scan at a fixed tempera-

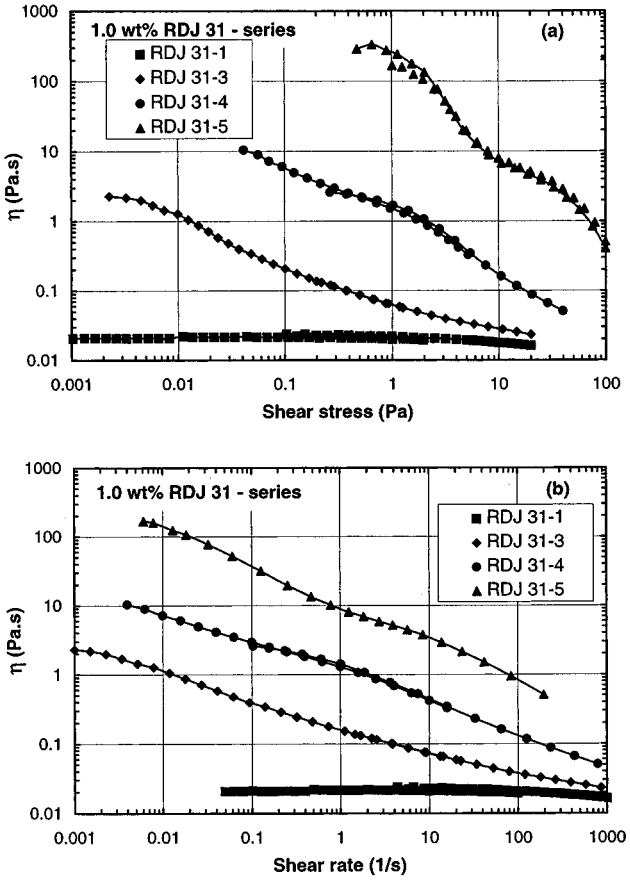

Figure 4. Steady shear viscosity of the 1 wt % solutions of RDJ31-series polymers: (a) as a function of shear stress; (b) as a function of shear rate.

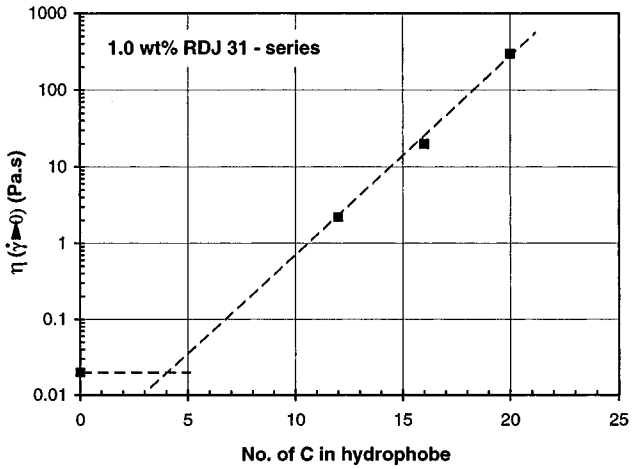

Figure 5. Plot of low shear viscosity of 1 wt % solutions of model associative HASE polymers as a function of hydrophobe chain length.

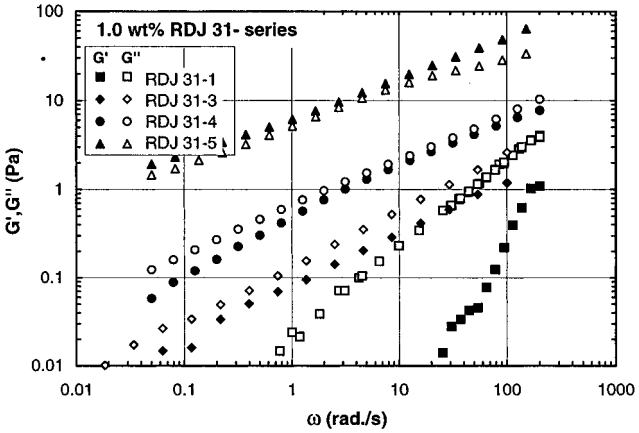

Figure 6. Dynamic storage and loss moduli of the 1 wt % solutions of RDJ31-series polymers.

ture, as is the case here, is expected to be lower than the activation enthalpy value that would have been obtained from Arrhenius plots.[20] The activation energy obtained from Arrhenius plots for HEUR type polymers have been found to be of the order of 1.8 kT per C atom of the hydrophobe,[20,27] while preliminary work on the HASE system indicates a value for comparable hydrophobe chain length to be about half this value. The variation found between the two types of associative polymers is probably due to the differences in the actual hydrophobicity of the associating groups (for the HASE polymers, the hydrophobe is attached directly to approximately 35 mol of rather hydrophilic ethylene oxide, while for the HEUR polymers the hydrophobic group is attached to an isocyanate group which can add to its hydrophobicity) and hence the aggregation number of the hydrophobic network junctions. Additionally, the association energy of the HASE polymers is found to increase with the length of the hydrophobic groups, as well as the concentration of the polymer in solution. The temperature effect on the flow behavior of model HASE polymers is under investigation at present.

From Figure 5, extrapolating the line of exponential dependence back to intercept the value for no-hydrophobe allows the determination of the minimum hydrophobe chain length below which no enhancement of viscosity due to hydrophobic association occurs. This is found to be in the vicinity of four carbon atoms. Further work with associative polymers containing lower hydrophobe chain lengths is being carried out to confirm this finding.

4.3. Viscoelastic Results. The linear viscoelastic properties of the associative polymers, including the one containing no hydrophobic macromonomer, are shown in Figure 6. For RDJ31-1, the loss modulus curve is proportional to ω while the storage modulus is proportional to ω^2, typical of a second-order fluid behavior. However, due to its low viscosity, the magnitude of the G' curve obtained may be subject to large errors and the effect of fluid inertia cannot be discounted.[28] While, on the contrary, for the three hydrophobe-containing polymers, the G' and G'' curves are almost parallel to each other and are of the same order of magnitude. However, the relative magnitude of the elastic to viscous components of each polymer is found to increase as the length of the hydrophobic group, and hence, the strength of the associating junctions, increases. A similar increase in the elastic component of the viscoelastic properties with increasing hydrophobe strength is also observed for the poly(acrylamide)s containing double C_6-alkyl chain hydrophobes compared to the single C_6-alkyl chain,[26] and for the alkali-soluble associative polymer containing complex, bulky hydrophobes in contrast to the simple alkyl chain.[1]

4.4. Viscoelastic Properties at Various Applied Stress Conditions. Using the technique of superposition of oscillation onto steady shear flows, the viscoelastic properties of the associative polymers at a number of applied shear stress conditions can be measured; these results can be plotted together as a function of frequency. A typical set of results for the associative polymer RDJ31-4 are shown in Figure 7. The overall behavior observed for the storage modulus and dynamic viscosity with increasing applied stress is similar to those obtained for RDJ31-5, which are shown as Figures 7, 8, and 10 in our previous paper.[15] With increasing applied stress beyond the zero-shear viscosity region, the network structure of the associative polymer is disrupted to such an extent that the G' values at low frequencies are greatly reduced, with the slope approaching second-order fluid behavior, while the dynamic viscosities approach steady values. This terminal region of the viscoelastic behavior is observed at higher and higher frequencies as the applied stress is increased. At higher frequencies in the transition region, the G' curves for the applied stress conditions are parallel to the normal G' curve with no applied stress, with the values being slightly higher with increasing applied stress. The dynamic viscosity curves in the transition region are also parallel to the normal η' curve and are slightly higher in value.

In the superposition of oscillation onto steady shear flow experiments, the steady shear viscosities obtained are constant and independent of frequencies (see Figure 7c); the viscosity at any applied stress value is found to be the same as the shear viscosity obtained from steady shear measurement. The agreement in the shear viscosity values obtained from superposition and from steady shear experiments is used as a benchmark test of the constant stress instrument and its accompanying software, for its ability to accurately resolve the output strain curves into their corresponding shear and oscillatory components. It also serves as an indication of the state of the polymer being tested, as viscosity values significantly different from those obtained in the normal steady shear tests could also indicate structural changes occurring in the polymer during testing.

From the results of superposition experiments, the relaxation time function for the associative polymers can be calculated with analogy to the Maxwell-type relaxation time, i.e. $\lambda(\tau_s,\omega) = G'(\tau_s,\omega)/\omega^2\eta'(\tau_s,\omega)$. The results for RDJ31-4 are shown in Figure 7d. Each of these relaxation time function curves shows a maximum that corresponds to the terminal region in the G' and η' curves; these maxima can be taken as an estimate of the longest relaxation time of the polymer at each of the applied stress conditions. In Figure 8 the relaxation time of the three associative polymers containing hydrophobes of various chain lengths are plotted as a function of shear stress. Shown on the same figure are the shear viscosity curves of the same three polymers. It is apparent that the relaxation time of the polymers shows a much larger decrease as the network structure is disrupted by shear, compared to the decrease in the viscosity. The stress required to reduce the relaxation time to the same value, of, e.g., 0.1 s, is increased by 1 order of magnitude as the polymer hydrophobe chain

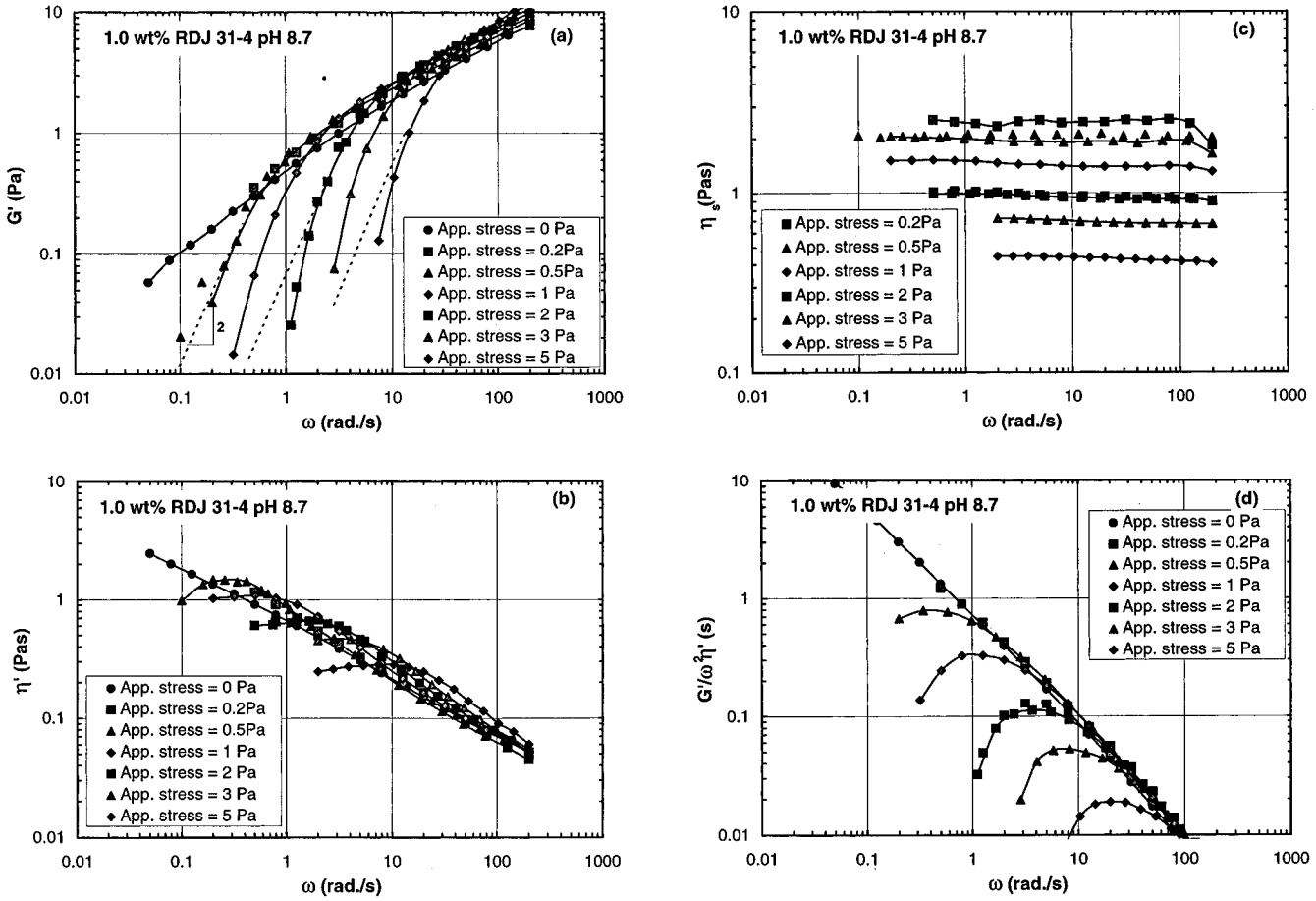

Figure 7. Results for the 1 wt % solution of RDJ31-4 obtained from superposition of oscillation on steady shear flows at various applied shear stresses: (a) storage modulus; (b) dynamic viscosity; (c) steady shear viscosity; (d) relaxation time function.

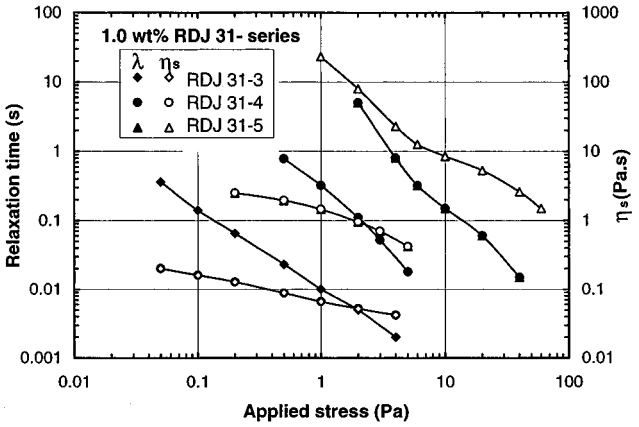

Figure 8. Relaxation time and shear viscosity of the 1 wt % solutions of RDJ31-series, as a function of applied shear stress.

length increases from C_{12} to C_{16}, and another order of magnitude from C_{16} to C_{20}. The relaxation time of the polymers in the low shear rate/stress region cannot be determined in this manner as the terminal region does not exist within the experimental frequency range (see Figures 9a, 10a, and 11a).

4.5. Fitting of Models to Experimental Results. Comparison of the storage and loss moduli curves at various applied shear stresses are shown for the polymers RDJ31-3, -4, and -5 in Figures 9−11, respectively. At no applied shear stress, the ratio between the elastic and viscous components increases as the hydrophobe chain length increases, as discussed previously. With increasing applied stress beyond the zero-shear viscosity value, the three associative polymers, all at a concentration of 1.0 wt % in aqueous solution at high pH, show distinctly different viscoelastic behaviors. The polymer RDJ31-3 displays a Zimm-like behavior (see Figure 9), with the G' curves showing a second-order behavior at low frequencies and the G' and G'' curves being parallel with a slope of $^2/_3$ at higher frequencies. With increasing applied stresses, the structure of the polymer network is continually being disrupted, and the terminal region of the polymer shifts toward higher frequencies, with the consequential reduction in its relaxation time, as can be seen in Figure 8. The curves of best fit of the Zimm theory to the measured G' and G'' data at different applied stresses can be determined, using a nonlinear regression analysis; the results are shown in Figure 9, while the model parameters λ_1 and G_0 for various applied stresses are given in Table 3a. Note that no Zimm model fitting of the unstressed condition is shown, as the terminal region of the data is not measurable within the frequency range of the experiments.

The linear viscoelastic properties of RDJ31-4 (see Figure 10), on the other hand show a distinctly Rouse-like behavior, with the G' and G'' curves being parallel and equal to each other with a slope of $^1/_2$ at high frequencies. Similar to the behavior observed for RDJ31-3, the terminal region shifts to higher frequencies, implying a decrease in the relaxation time of the polymer as the network is being disrupted by increasing applied stress. Also shown in Figure 10 are the best fit curves of the Rouse theory to the data, with the model parameters λ_1 and G_0 listed in Table 3b.

The G' and G'' data of RDJ31-3 at different applied stresses are reduced according to eqs 3 and 4, respec-

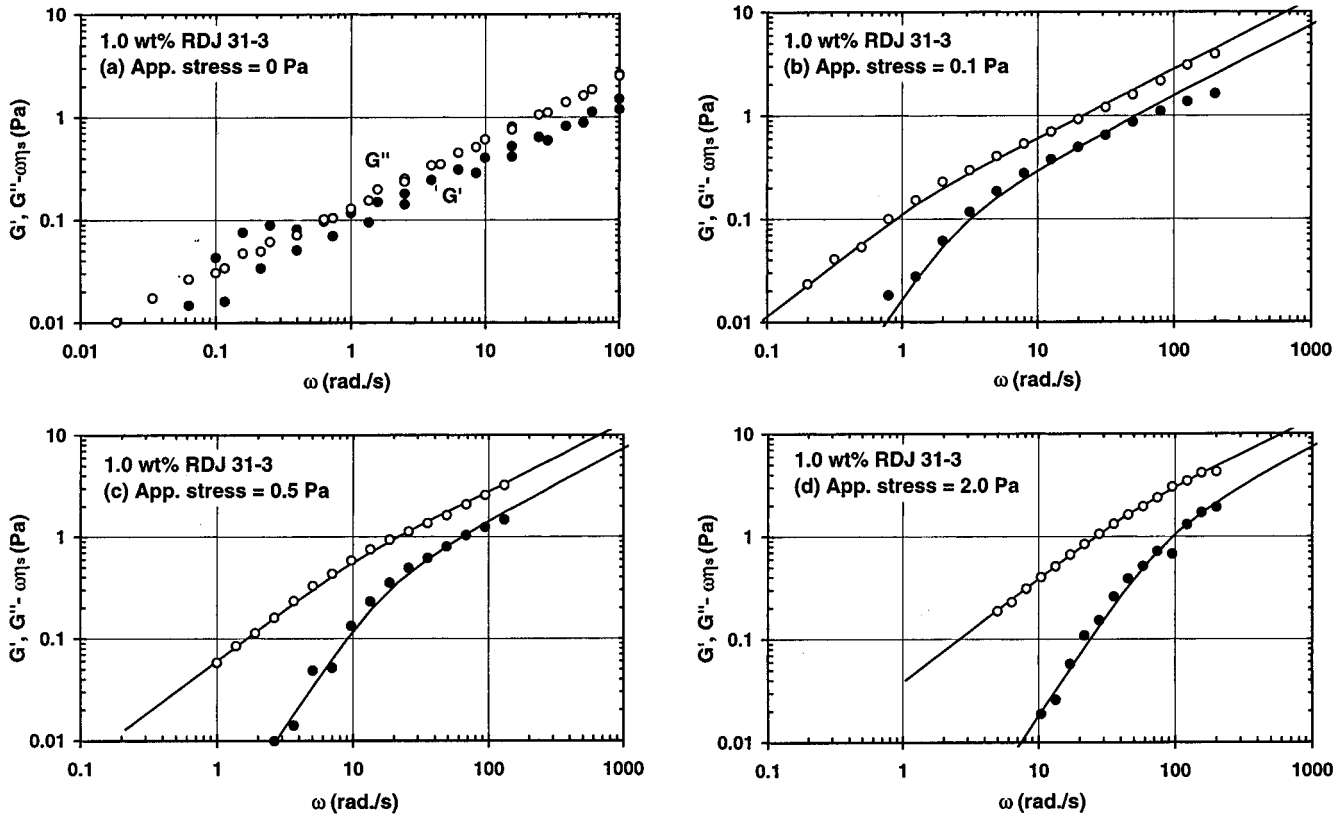

Figure 9. Storage and loss moduli of the 1 wt % solution of RDJ31-3 and the Zimm model fit at an applied stress of (a) 0 Pa, (b) 0.1 Pa, (c) 0.5 Pa, and (d) 2 Pa.

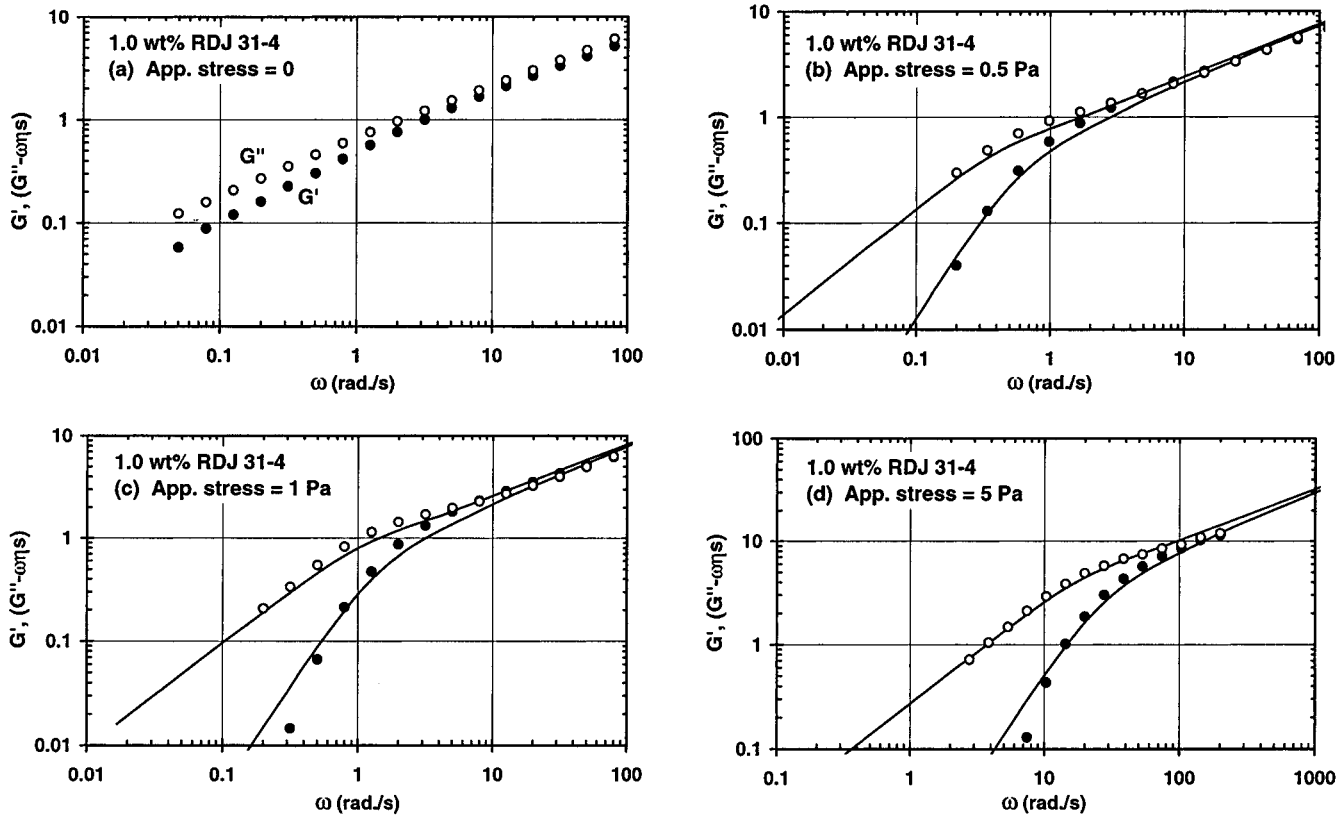

Figure 10. Storage and loss moduli of the 1 wt % solution of RDJ31-4 and the Rouse model fit at an applied stress of (a) 0 Pa, (b) 0.5 Pa, (c) 1 Pa, and (d) 5 Pa.

tively, using the parameters shown in Table 3a, and the results are compared with the Zimm master curves[5] in Figure 12a. Similarly for RDJ31-4 using the parameters given in Table 3b, the results are shown and compared with the Rouse master curves[5] in Figure 12b. For the two polymers the reduced data at different applied stress conditions all follow the Zimm/Rouse behavior for most of the range of frequencies measured.

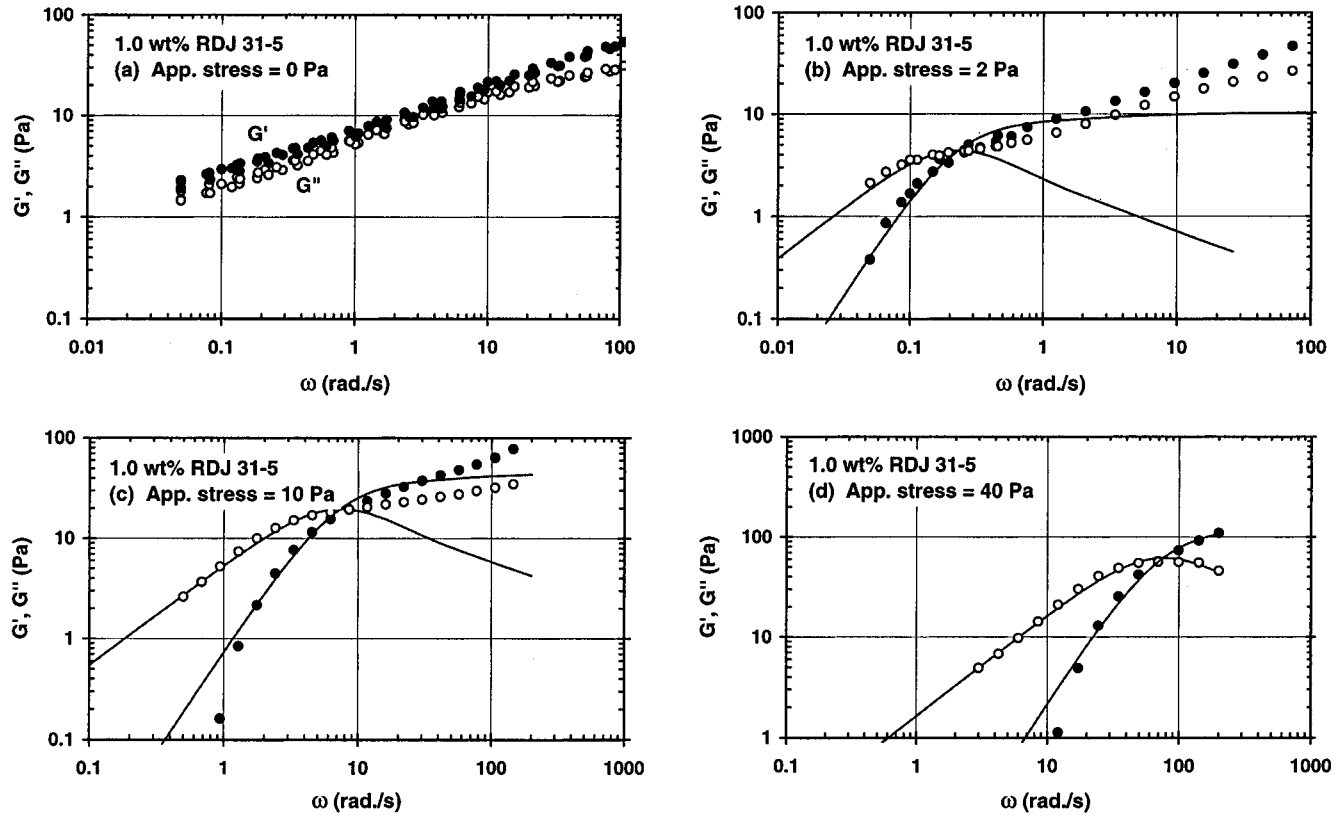

Figure 11. Storage and loss moduli of the 1 wt % solution of RDJ31-5 and the Doi−Edward model fit at an applied stress of (a) 0 Pa, (b) 2 Pa, (c) 10 Pa, and (d) 40 Pa.

Table 3. Relaxation Time and Modulus Values at Various Applied Stresses

(a) Zimm (First Mode) Values for RDJ31-3

	applied stress (Pa)						
	0.05	0.1	0.2	0.5	1.0	2.0	5.0
λ_1 (s)	0.87	0.32	0.13	0.047	0.021	0.0096	0.0039
G_0 (Pa)	0.078	0.15	0.28	0.55	0.96	1.70	3.48

(b) Rouse (First Mode) Values for RDJ31-4

	applied stress (Pa)					
	0.2	0.5	1.0	2.0	3.0	5.0
λ_1 (s)	4.15	1.45	0.60	0.20	0.096	0.031
G_0 (Pa)	0.32	0.58	0.97	1.80	2.76	5.29

(c) Doi−Edwards Model Values for RDJ31-5

	applied stress (Pa)						
	2	4	6	10	20	40	60
λ_1 (s)	14.45	0.71	0.27	0.14	0.057	0.013	0.006
G_0 (Pa)	10.6	23.0	34.3	47.4	78.7	149.2	203.4

For RDJ31-3, a slight deviation from the slope of $^2/_3$ is observed at the highest frequencies, whereas for RDJ31-4, there is a deviation from the slope of 2 in the low-frequency end. Thus, RDJ31-3 shows a general Zimm-type behavior and RDJ31-4 a Rouse-like behavior when their structures are sufficiently disrupted from their equilibrium states due to shear.

For RDJ31-5, its viscoelastic behavior under various shear conditions (see Figure 11) is quite different from those of the other two associative polymers. When sheared with a stress in excess of 2 Pa, i.e. beyond the zero-shear rate region, the storage modulus is again greatly reduced and approaches second-order behavior at low frequencies. At higher frequencies the G' and G'' curves cross each other and G' becomes larger than

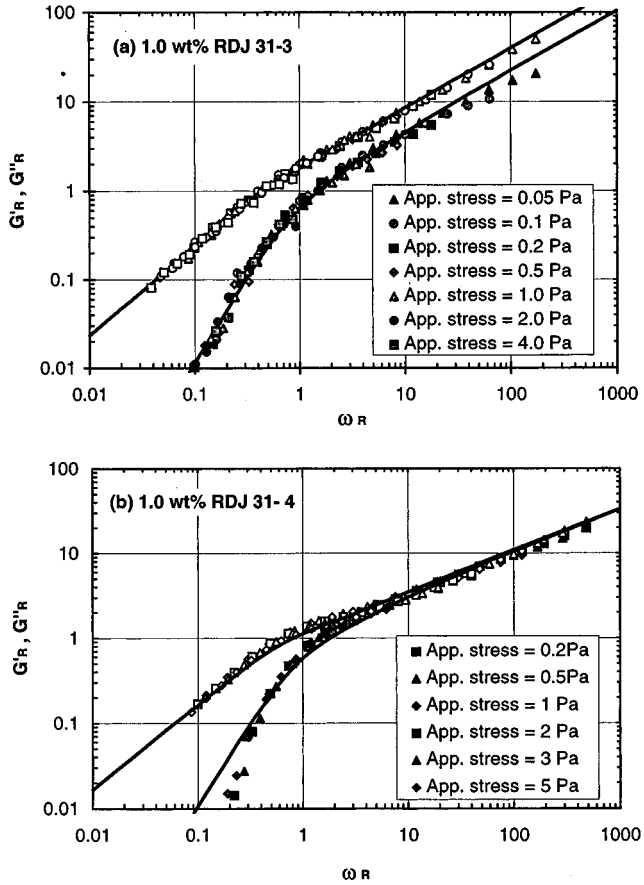

Figure 12. Reduced storage and loss moduli of (a) the 1 wt % solution of RDJ31-3 and the Zimm model master plot and (b) the 1 wt % solution of RDJ31-4 and the Rouse model master plot.

G''. The viscoelastic data for RDJ31-5 have been fitted with the Doi−Edwards reptation model, and the results are shown in Figure 11. The reptation theory of Doi−Edwards does not fit the high-frequency behavior of this polymer, clearly indicating that other modes of relaxation need to be incorporated in the model. However, the magnitude of the relaxation time and modulus obtained provides a useful comparison with the values for RDJ31-3 and -4, obtained from the Zimm and Rouse model fits; these parameters are given in Table 3c.

5. Discussion

For all three associative polymers under normal oscillation conditions, i.e. without applied shear stress, it was not possible to measure using the existing rheometers to low enough frequencies to determine the terminal viscoelastic region of the fluid. Hence, it is uncertain whether the Zimm or Rouse-type behavior would still be pertinent in the unperturbed state for RDJ31-3 and -4, respectively. This seems unlikely to be the case from later results obtained from a freshly prepared sample of RDJ31-4, which was tested within 2 weeks of preparation. The results showed that, while the loss modulus values are similar, the storage moduli are significantly higher compared to the aged sample presented here, although the overall Rouse-type behavior is still observed with increasing applied stress. The increase in G' values is particularly significant in the unperturbed state, as at the low-frequency end G' of the fresh sample is actually higher than the corresponding G'' values. The drop in the elastic component of the aged sample is probably due to a reduction in the amount of hydrophobic associations caused by hydrolysis and cleavage of some hydrophobe−ethylene oxide side chains from the methacrylic acid−ethyl acrylate backbone. The consequence is not only a drop in viscosity but, more significantly, a significant decrease in the elastic properties of the sample.

For all three associative polymers, the effect of increasing applied stress has been to shift the terminal region to higher frequencies, while the behavior in the transition zone remains essentially unaffected. Thus, it is the longest relaxation time of the spectrum that is being curtailed as the polymer network is disrupted. The dynamics of network with temporary or reversible junctions are considered by a number of authors.[29,30] Leibler et al.'s hindered reptation model[29] is similar to the Doi−Edwards' theory, which also predicts two basic relaxation processes. The slower process is related to the reptation motion of the polymer chains by coherent breaking of a few cross-link points at a time and is found to be a function of the degree of associations. The faster process is due to relaxation of segments between entanglement points and is related to the average lifetime of an association. For this fast relaxation process, both Rouse[29] and Zimm[30] type spectra have been utilized.

The absence of a terminal region in the experimental frequency range for the associative polymers in the unstressed state suggests the existence of a much longer relaxation process, possibly associated with the reptation-type motion of the polymer chains. Hence a terminal region is expected at a much lower frequency range. Applying an increasing stress to disrupt the polymer network would drastically curtail the longest relaxation times, as a result of a reduction in the junction density, while the short relaxation spectrum remains unaffected. The short relaxation time spectrum, which is a function of the lifetime of the associations or network junctions, is thus related to the strength of the associations and the hydrophobe chain length. This manifestation can be observed as a change from Zimm-like to Rouse-like behavior as the length of the hydrophobe chain increases from 12 to 16 carbon atoms, and to one with a crossover between the G' and G'' curves (i.e., reptation-type) as the number of carbon atoms of the hydrophobes increases further to 20. The major difference among these three models is in the distribution of the relaxation times, with the Zimm theory comprising the most closely spaced terms, followed by Rouse and then Doi−Edwards. This difference may be due to a decrease in the number of hydrophobes involved in each associating junction as the hydrophobe chain length increases; this conjecture remains to be confirmed using the fluorescence techniques.

In the Rouse and Zimm theories, the relaxation modulus G_0 term is given by $G_0 = cRT/M$, where c is the concentration of the polymer in solution and M is the molecular weight. From Table 3a−c, it can be seen that G_0 increases with applied stress for all the associative polymers, and hence the molecular weight term decreases for a fixed polymer concentration, as expected. For associative polymers with hydrophobes forming temporary junctions with neighboring polymer chains, one may visualize an "effective" molecular weight which encompasses several polymer chains and is proportional to the degree of network junctions. As the structure of the network is destroyed by increasing applied stress, the junction density is reduced, thus resulting in a decrease in the effective molecular weight. This picture of the network system of HASE polymers awaits further confirmation and refinement.

6. Conclusions

The associative polymers form a network of temporary junctions of associating hydrophobic ends. The hydrophobic association increases in strength with increasing hydrophobe chain length. The difference in the strength of the hydrophobic associations affects both the association number, i.e. the number of the hydrophobes associating to form network junctions, and the junction density. The steady shear viscosity of the three associative polymers varies over three decades of magnitude as the hydrophobe chain length increases from C_{12} to C_{20}. For each polymer in the unsheared state, their viscoelastic elastic and viscous components are similar in magnitude, but the ratio of the elastic to viscous parts increases from a value below 1 to above 1 as the hydrophobe chain length, and hence the association strength, increases. When the network is disrupted from its equilibrium state by an applied stress beyond the zero-shear viscosity region, these three polymers show distinctly different viscoelastic behavior, from a Zimm-like to Rouse-like, to one with crossover in the G' and G'' curves. This difference may be interpreted in terms of the difference in the distribution of the relaxation times among these three molecular theories. Moreover, the failure to observe the terminal region of the unstressed state in the experimental frequency range strongly suggests that other long characteristic times may be involved in the relaxation process.

7. Acknowledgments

The authors would like to acknowledge the important role of Drs. Mel Farmer and Dave Bassett in promoting the collaboration between Union Carbide and NTU on

this project. The authors also had several useful discussions with Dr. Peter Farrington on the interpretation of the results in terms of the relaxation time distribution. The financial support in the form of a RDAS grant by the National Science and Technology Board of Singapore is gratefully acknowledged.

8. References

(1) Jenkins, R. D.; DeLong, L. M.; Bassett, D. R. In *Hydrophilic Polymers: Performance with Environmental Acceptability*; Glass, J. E., Ed.; ACS Symposium Series No. 248; American Chemical Society: Washington, DC, 1996; Chapter 23, p 425.
(2) Aubry, T.; Moan, M. *J. Rheol.* **1994**, *38* (6), 1681.
(3) Rouse, P. E., Jr. *J. Chem. Phys.* **1953**, *21* (7), 1272.
(4) Zimm, B. H. *J. Chem. Phys.* **1956**, *24* (2), 269.
(5) Ferry, J. D. *Viscoelastic Properties of Polymers*, 3rd ed.; Wiley: New York, 1980.
(6) Zimm, B. H.; Roe, G. M.; Epstein, L. F. *J. Chem. Phys.* **1956**, *24* (2), 279.
(7) (a) DeMallie, R. B., Jr.; Birnboim, M. H.; Frederick, J. E.; Tschoegl, N. W.; Ferry, J. D. *J. Phys. Chem.* **1962**, *66*, 536. (b) Frederick, J. E.; Tschoel, N. W.; Ferry, J. D. *J. Phys. Chem.* **1964**, *68*, 1974. (c) Holmes, L. A.; Ferry, J. D. *J. Polym. Sci.* **1968**, *C23*, 291.
(8) Tam, K. C. Ph.D. Thesis, Monash University, Melbourne, 1990.
(9) Holmes, L. A.; Kusamizu, S.; Osaki, K.; Ferry, J. D. *J. Polym. Sci., Polym. Phys. Ed.* **1971**, *9*, 2009.
(10) DeGennes, P. G. *J. Chem. Phys.* **1971**, *55*, 572.
(11) Doi, M.; Edwards, S. F. *The Theory of Polymer Dynamics*; Clarendon Press: Oxford, U.K., 1986.
(12) Guo, L. First Year Report, Nanyang Technological University, 1996.
(13) Brandrup, J.; Imergut, E. H. *Polymer Handbook*, 3rd ed.; John Wiley: New York, 1989.
(14) Boris, D. C.; Colby, R. H. *Proceedings of the 12th International Congress on Rheology*; Laval University: Quebec City, Canada, 1996; p 195.
(15) Tirtaatmadja, V.; Tam, K. C.; Jenkins, R. D. Submitted to *Macromolecules* **1997**, *36*, 1426.
(16) Kumacheva, E.; Rharbi, Y.; Winnik, M. A.; Guo, L.; Tam, K. C.; Jenkins, R. D. *Langmuir* **1997**, *13*, 182.
(17) Alami, E.; Almgren, M.; Brown, W.; Francois, J. *Macromolecules* **1996**, *29*, 2229.
(18) Xu, B.; Yekta, A.; Li, L.; Masoumi, Z.; Winnik, M. A. *Colloid Surf.* **1996**, *112*, 239.
(19) (a) Francois, J. *Prog. Org. Coat.* **1994**, *24*, 67. (b) Francois, J.; Maitre, S.; Isel, F. *Colloid Surf. A* **1996**, *112*, 251.
(20) Annable, T.; Buscall, R.; Ettelaie, R.; Whittlestone, D. J. *J. Rheol.* **1993**, *37*, 695.
(21) Fonnum, G.; Blakke, J.; Hansen, F. K. *Colloid Polym. Sci.* **1993**, *271*, 380.
(22) Jenkins, R. D. Ph.D. Thesis, Lehigh University, Bethlehem, 1990.
(23) Tam, K. C.; Farmer, M. L. *Proceedings of the 7th National Conference on Rheology*; University of Queensland: Brisbane, Australia, 1994, p 211.
(24) Ross-Murphy, S. B.; Shatwell, K. P. *Biorheology* **1993**, *30*, 217.
(25) Schultz, J. M. The Mechanics of Amorphous Polymers. In *Polymer Materials Science*; Prentice-Hall: Englewood, Cliffs, NJ, 1974; Chapter 7.
(26) Volpert, E.; Selb, J.; Candau, F. *Macromolecules* **1996**, *29*, 1452.
(27) Tarng, M.-R.; Kaczmarski, J. P.; Lundberg, D. J.; Glass, J. E. In *Hydrophilic Polymers: Performance with Environmental Acceptability*; Glass, J. E., Ed.; ACS Symposium Series No. 248; American Chemical Society: Washington, DC, 1996; Chapter 17, p 305.
(28) Walters, K. *Rheometry*; Chapman and Hall: London, 1975.
(29) Leibler, L.; Rubenstein, M.; Colby, R. H. *Macromolecules* **1991**, *24*, 4701.
(30) Groot, R. D.; Agterof, G. M. *Macromolecules* **1995**, *28*, 6284.

MA961202B